Orbital implants and prostheses: postoperative computed tomographic appearance.

M E Gale, M E Vincent and F C Sutula

AJNR Am J Neuroradiol 1985, 6 (3) 403-407
http://www.ajnr.org/content/6/3/403

Orbital Implants and Prostheses: Postoperative Computed Tomographic Appearance

M. Elon Gale[1]
Miriam E. Vincent[1]
Francis C. Sutula[2]

Computed tomographic (CT) scans of 19 patients with 10 right and nine left orbital implants were reviewed. Except for orbital soft-tissue swelling due to recent surgery or infection, CT scans obtained with both the implant and prosthesis in place showed relative symmetry of the postoperative side and the native globe. Benign air collections were often associated with either the implant or prosthesis interface or with seating of the prosthesis in the conjunctival fornices. Six patients had either cartilage, silicone, or glass beads placed surgically along the orbital floor to elevate the implants, four having had prior depressed orbital floor fractures. CT identified implant migration in five patients. The orbital prosthesis, usually constructed of solid methylmethacrylate, is fitted over the implant and simulates the appearance of the eye of the contralateral side. The operative anatomy and its relation to the CT appearance of the implant and external prosthesis are reviewed.

Computed tomographic (CT) scanning is widely used for evaluation of the orbits. Primary and secondary neoplasms, posttraumatic anatomy, orbital pseudotumor, and adjacent lacrimal gland abnormalities are well described in the literature [1–4]. Exophthalmos and muscular thickening associated with Graves disease present a characteristic CT appearance [5]. We have found CT to be useful in the evaluation of the orbit before and after enucleation with operative reconstruction. This reconstruction entails surgical placement of a spherical implant in place of the native globe, followed postoperatively by creation of a lens-shaped removable prosthesis designed to match the contour of the contralateral sclera. The prosthesis is hand-painted to simulate the color and detail of the patient's normal iris, pupil, and sclera. The CT appearance of the normal postoperative orbital implant and of the potential complications are described in this report. The radiologic appearance is based on an understanding of orbital anatomy and surgical technique.

Materials and Methods

In a retrospective review encompassing a 6-year period, we evaluated 28 CT scans of the orbits or brain in 19 patients with orbital implants, for the presence of exophthalmos, periprosthetic or palpebral air, and migration or extrusion of the implant. In those cases where material was used to support the implant, the type of material and its relation to the normal or deformed orbital floor and walls was noted. Scans were obtained at widely variable periods postoperatively, from days to years, depending on the clinical problem. Orbital CT studies were performed to document the presence and type of implant, to confirm the clinical suspicion of implant migration, to determine the appropriateness of implant size relative to the bony orbit, or to exclude implant breakage. Six patients had multiple scans, usually to evaluate a neurologic problem unrelated to the orbital surgery.

Results

In all cases the center of the implant was recessed posteriorly in the orbit as

Received May 30, 1984; accepted after revision October 11, 1984.

Presented at the annual meeting of the American Society of Head and Neck Radiology, San Antonio, May 1984.

[1] Department of Radiology, Tufts University School of Medicine, Boston, MA 02111, and Veterans Administration Medical Center, 150 S. Huntington Ave., Boston, MA 02130. Address reprint requests to M. E. Gale.

[2] Department of Ophthalmology, Tufts University School of Medicine, and Veterans Administration Medical Center, Boston, MA 02130.

AJNR 6:403–407, May/June 1985
0195–6108/85/0603–0403

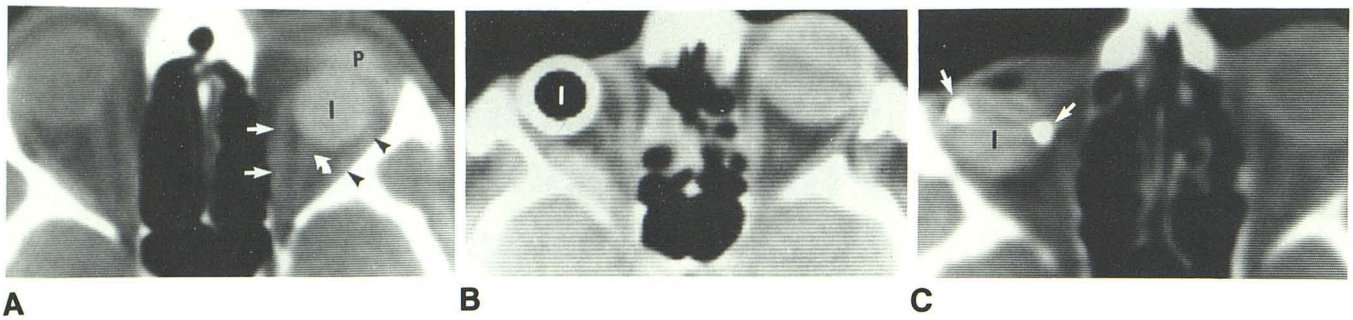

Fig. 1.—**A**, Homogeneous methylmethacrylate implant (I) is properly positioned between medial (*straight arrows*) and lateral (*arrowheads*) rectus muscles and anterior to optic nerve (*curved arrow*). Methylmethacrylate prosthesis (P) is well seated anteriorly. **B**, Hollow glass implant contains central air. No prosthesis was in place during CT imaging, highlighting relative posterior location of implant itself. **C**, CT image through orbit shows peripheral wire mesh (*arrows*) that rings implant.

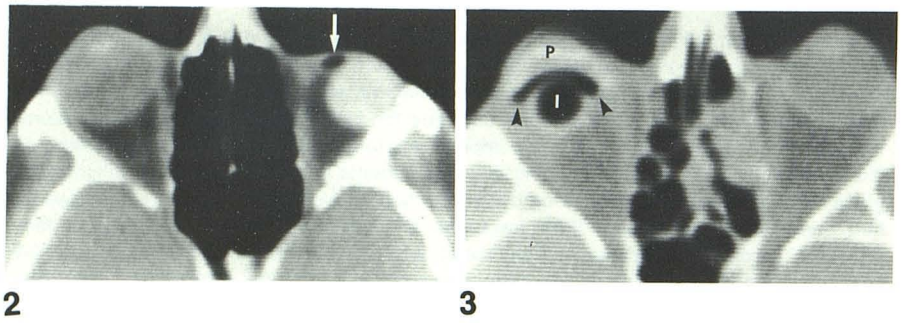

Fig. 2.—Small air bubble (*arrow*) trapped between eyelids medial to implant.

Fig. 3.—Benign curvilinear air collection (*arrowheads*) between prosthesis (P) and hollow glass implant (I). Relative bilateral symmetry with prosthesis in place.

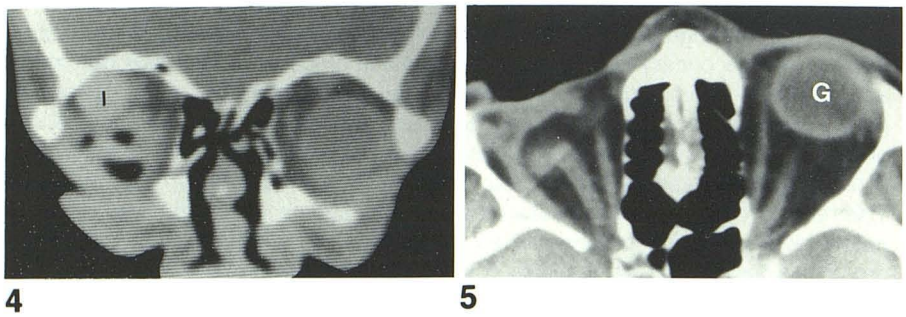

Fig. 4.—Coronal CT scan. Orbital implant (I) lies superolateral to muscular cone, and hence outside of Tenon capsule. Air and soft-tissue swelling inferior to implant is from infection.

Fig. 5.—Right orbital implant is not in proper position on axial CT scan through both optic nerves and near equator of left globe (G). It had migrated inferiorly below scan plane, leaving only its superior surface partly imaged. Coronal scan was not obtained.

compared with the contralateral globe (fig. 1). In 17 cases in which scanning was performed with the prosthesis in place, symmetry of the orbit was restored in all but three scans. One patient who had orbital soft-tissue infection and two patients who had recent operations demonstrated relative exophthalmos.

Eight of the 10 scans obtained with the prosthesis removed demonstrated air trapped between the eyelids (fig. 2). Twelve of the 17 scans obtained with the prosthesis in place showed air between the prosthesis and the implant (fig. 3). In only one instance was the presence of air related to infection (fig. 4). In this case, associated soft-tissue swelling and edema of orbital fat were also evident. In one case, radial artifacts from metal in the implant obscured accurate determination of the presence of a prosthesis and periprosthetic or palpebral air.

Migration of the orbital implant was diagnosed on eight scans in five patients (fig. 5). In these cases, a large part of the implant was extraconal. In one other case, only a small part of the implant appeared extraconal, hence the presence of migration was indeterminate.

In four of six cases where supporting material was present, it was used to correct prior traumatic deformity and depression of the orbital floor. In the other two cases without prior orbital floor fracture, the support material was placed to correct superior sulcus deformities alone. The support material was always located in the extraconal space along the inferior, inferolateral, or inferomedial aspect of the bony orbit (figs. 6 and 7).

Discussion

Understanding the CT appearance of normal orbital implants and prostheses requires knowledge of implant materials, orbital anatomy, and surgical technique. The implant

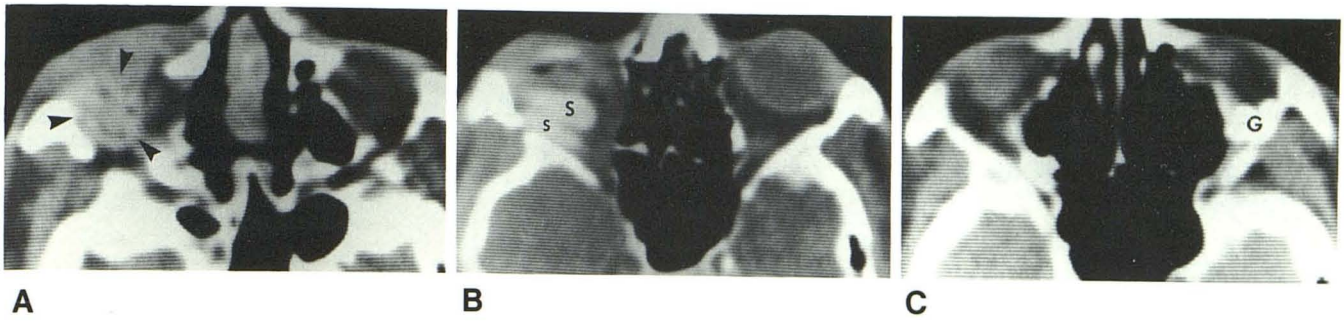

Fig. 6.—**A**, Recently placed heterogeneous collection of diced cartilage (*arrowheads*) is clearly identified along orbital floor. Postoperative soft-tissue swelling anterior to cartilage. **B**, Smoothly marginated, homogeneous pieces of silicone (S) lying along inferior posterior orbit elevated implant from below. **C**, Lobular collection of dense glass beads (G) along orbital floor.

Fig. 7.—**A**, Dense lobular glass beads (*arrowheads*) lie along lateral orbital wall in posterior orbital coronal CT scan. **B**, Coronal CT scan through muscle cone posterior to implant and globe. Inferomedial piece of silicone (S) supporting fractured floor and mirroring contralateral intact orbital floor.

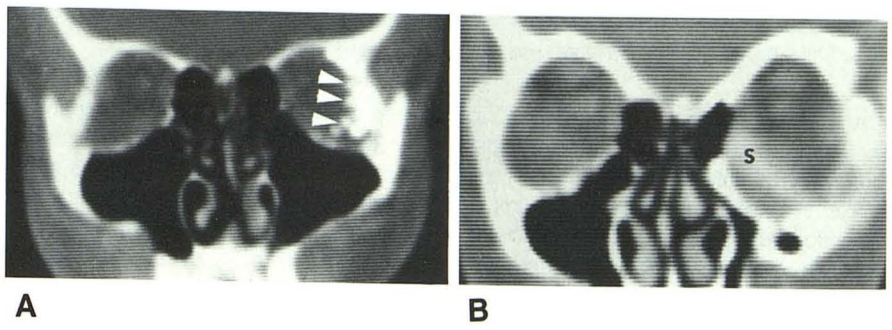

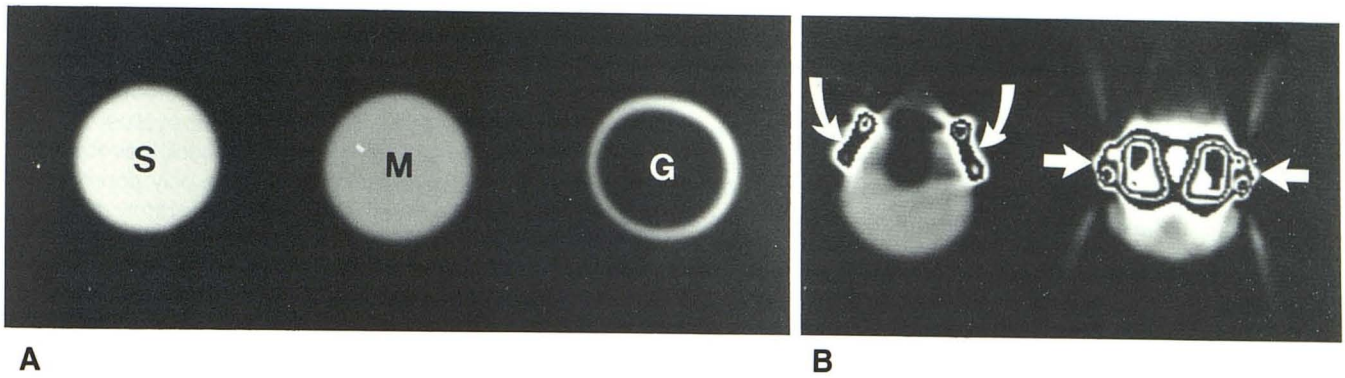

Fig. 8.—Density of silicone implant (S) measured about 440 H, that of methylmethacrylate (M) about 135 H, and that of wall of glass (G) shell about 520 H. **B**, Wire mesh (*curved arrows*) surrounds implant. CT artifacts are generated by extremely dense magnet (*straight arrows*) in this older implant. It is photographed here at maximum window width to suppress these artifacts.

density on CT depends on its composition (fig. 8). Spherical implants are constructed of titanium, glass, silicone, and methylmethacrylate, in order from most to least dense on CT. The exact density of the latter two is variable, however, and depends in part on the manufacturing process. Many glass implants are centrally hollow, having only a thin peripheral glass shell. In these, CT demonstrates a large central sphere of air density surrounded by a ring of high attenuation. Some implants have a peripheral metallic mesh ring used to attach the extraocular muscles. A few older models contain anteriorly placed metal magnets. These irregularly contoured metals may produce significant CT artifacts that obscure adequate visualization of the entire orbit.

Tenon capsule, the fascia bulbi, is a thin membrane that surrounds the sclera of the native globe [6, 7]. It invests the attachments of the rectus muscles to about a third of their anterior length. Posteriorly, the optic nerve penetrates a round defect in the capsule. Anteriorly, a second defect in the capsule marginates the cornea. Movement of the globe by the extraocular muscles is transmitted not only by direct muscular attachment to the globe, but also in part by muscular attachment to this membranous capsule. The extraocular muscles and the intermuscular membrane that lie between them define the orbital cone. However, since neither Tenon capsule nor the intermuscular membrane are thick enough to be identifiable on CT, their location is inferentially determined.

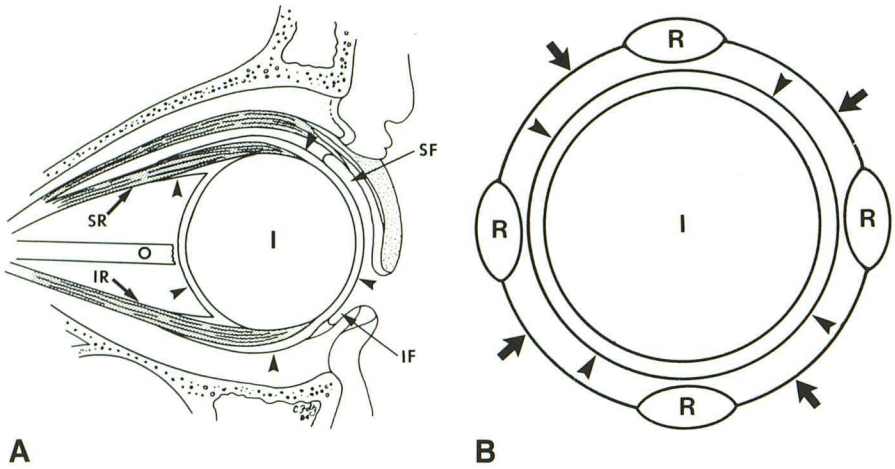

Fig. 9.—**A**, Sagittal diagram through normal postoperative orbit. Implant (I), inferior (IR) and superior (SR) rectus muscles, optic nerve (O), inferior (IF) and superior fornices (SF), and Tenon capsule (*arrowheads*). **B**, Coronal diagram posterior to implant (I) equator. Rectus muscles (R), intermuscular membrane (*arrows*), and circumferential nature of Tenon capsule (*arrowheads*).

After enucleation of the damaged or diseased globe, the implant is cradled within Tenon capsule [8] (fig. 9). The muscular attachments are left intact and the anterior defect in Tenon capsule is closed. The implant thereby prevents retraction of the extraocular muscles. Often the posterior defect is closed as well to avoid migration of the implant from its intracapsular location. Since each defect is closed by approximation of its margins, the volume contained within the postoperative capsule is less than that in the normal intracapsular space. Hence, the appropriate sized implant will appear smaller on CT than the contralateral native globe. Too large an implant may rupture or erode through Tenon capsule, and come to lie in an extraconal location.

Since the implant is smaller than the native globe, the implant always comes to lie posteriorly in the bony orbit, often associated with a superior sulcus deformity. This latter deformity, a soft-tissue depression of the upper eyelid above the implant and below the superior orbital rim, is also a result of the relatively undersized implant occupying an inferior location within the bony orbit. Implantation of materials such as diced cartilage, silicone, or glass beads along the orbital floor raises the level of the implant relative to the bony orbit. This cosmetically equalizes the central points of the implant-prosthesis complex and the native eye and decreases the superior sulcus deformity, whether or not there has been prior floor fracture and depression. Since glass beads occasionally move within the orbit and even out through the orbital fissures, their use has generally been abandoned.

CT allows easy identification of the composition of floor support material. Diced cartilage is not as dense as bone, has irregular contours, and is somewhat heterogeneous, becoming more homogeneous with age. Silicone has a slightly higher density than cartilage, and is very homogeneous with smooth margins. Glass beads are round, small, and very dense.

An orbital prosthesis that simulates the appearance of the eye of the contralateral side is fitted over the implant. Virtually all prostheses are constructed of solid methylmethacrylate and have similar density on CT. Rarely, a large prosthesis may be hollow or glass, and therefore have an appropriately different density. In the past, many prostheses were held in place by integration with the implant using posts or magnets. Current nonintegrated prostheses are lodged behind the eyelids in the superior and inferior conjunctival fornices. This prevents the prosthesis from falling out, while the relatively posterior implant prevents the prosthesis from moving too deep within the orbit. Motion is transmitted to the prosthesis from the extraocular muscles via the conjunctivae and, to a lesser extent, via the implant itself.

The proper curvature of the prosthesis approximates the contour of the contralateral native eye. Thus, there is often a discrepancy between the arc of curvature of the wide posterior prosthetic surface and that of the smaller implant enclosed in the Tenon capsule. Within this gap, air is often identified on the CT scan. Similarly, distortion of the eyelids with or without the prosthesis in place may cause benign air trapping in the fornices. These collections of air are only appreciated on CT and are of no clinical significance. Only rarely does the presence of air indicate infection. In the single patient where air was associated with infection, air was not only present in the usual location between the prosthesis and implant, but also lateral to the prosthesis. In cases where air is present in an atypical location, particularly when associated with soft-tissue swelling, infection should be strongly considered.

Direct coronal CT or coronal reconstructions are often helpful to identify the relative positions of the support material, the implant, and the orbital muscle cone within the bony orbit as compared with the contralateral side [9]. Coronal CT is ideal for recognition of implant migration since it shows the implant position relative to the muscle cone. If a large part of the implant lies outside adjacent recti, extracapsular migration most likely has occurred. Since the intermuscular membrane is relatively lax, an implant located partly outside the adjacent muscles may remain within the Tenon capsule by displacing the intermuscular membrane before it. A prosthesis may not seat properly when positioned over an implant that has migrated. However, only CT can confirm the suspected diagnosis of migration, since the implant may not be easily palpated due to the surrounding orbital bone and overlying superficial scar tissue. Surgical revision may be required to relocate the implant to correct the cosmetic appearance.

In summary, CT is excellent for the postoperative evaluation of orbital implants and prostheses. CT clearly identifies the type of implant and the precise location of supporting floor material used to correct superior sulcus deformity. Furthermore, CT is the method of choice to confirm and characterize the degree and direction of implant migration after rupture from Tenon capsule.

REFERENCES

1. Forbes GS, Earnest F IV, Waller RR. Computed tomography of orbital tumors, including late-generation scanning techniques. *Radiology* **1982**;142:387–394
2. Hammerschlag SB, Hughes S, O'Reilly GV, Naheedy MH, Rumbaugh CL. Blow-out fractures of the orbit: a comparison of computed tomography and conventional radiography with anatomical correlation. *Radiology* **1982**;143:487–492
3. Harr DL, Quencer RM, Abrams GW. Computed tomography and ultrasound in the evaluation of orbital infection and pseudotumor. *Radiology* **1982**;142:395–401
4. Balchunas WR, Quencer RM, Byrne SF. Lacrimal gland and fossa masses: evaluation by computed tomography and A-mode echography. *Radiology* **1983**;149:751–758
5. Enzmann DR, Donaldson SS, Kriss JP. Appearance of Graves' disease on orbital computed tomography. *J Comput Assist Tomogr* **1979**;3:815–819
6. Williams PL, Warwick R, eds. The accessory visual apparatus. In: *Gray's anatomy*, 36th edition. New York: Saunders, **1980**:1178–1184
7. Wolff E. The extrinsic muscles of the eye. In: Last RJ, ed. *Anatomy of the eye and orbit*. Philadelphia: Saunders, **1968**:265–271
8. Parr GR, Goldman BM, Rahn AO. Surgical considerations in the prosthetic treatment of ocular and orbital defects. *J Prosthet Dent* **1983**;49:379–385
9. Schwarz GS, Kirshner H, Messina AV. Computed tomographic scanning for locating an emplaced plastic orbital plate. *Ann Ophthalmol* **1982**;14:761–762